Formation, Manipulation, and Elasticity Measurement of a Nanometric Column of Water Molecules

H. Choe,[1,2] M.-H. Hong,[1,2] Y. Seo,[2] K. Lee,[1] G. Kim,[1] Y. Cho,[1] J. Ihm,[1] and W. Jhe[1,2,*]

[1]*School of Physics, Seoul National University, Seoul 151-747, Korea*

[2]*Center for Near-Field Atom-Photon Technology, Seoul National University, Seoul 151-747, Korea*

(Received 21 March 2005; published 28 October 2005)

Nanometer-sized columns of condensed water molecules are formed by an atomic-resolution force microscope operated in ambient conditions. An unusual stepwise decrease of the force gradient associated with the ultrathin water bridge in the tip-substrate gap is observed during its stretch, exhibiting regularity in step heights (≈ 0.5 N/m) and plateau lengths (≈ 1 nm). Such ''quantized'' elasticity is indicative of an atomic-scale stick slip at the tip-water interface. A thermodynamic-instability-induced rupture of the water meniscus (5 nm long and 2.6 nm wide) is also found. This work opens a high-resolution study of the structure and interface dynamics of a nanometric aqueous column.

DOI: 10.1103/PhysRevLett.95.187801 PACS numbers: 62.10.+s, 07.79.Lh, 47.17.+e

Water is one of the most important substances of life and has been studied extensively for hundreds of years. Nonetheless, it is still quite a unique material that keeps surprising us and exhibits peculiarities, in particular, when confined in a nanometric configuration. For example, water and simple organic liquids exhibit solidlike orderedness in molecularly thin films [1–3]. Water molecules inside hydrophobic nanotubes manifest phases of ice that are not found under bulk conditions [4]. However, since bulk water possesses only short-range order [5] and water molecules move incessantly, it is usually difficult to experimentally investigate novel features of confined water structures other than thin films.

In this Letter, we have employed an atomic-resolution noncontact atomic force microscope (AFM) in air [6] and achieved the spontaneous formation of a nanometric liquid column consisting of thousands of water molecules. We also have performed the sensitive measurement of the elastic property (or the force gradient) of the thin water column during its mechanical stretch. We have thereby demonstrated several novel phenomena: (i) unusual stepwise decrease of the force gradient, associated with the atomic-scale stick slip on the AFM-tip surface, (ii) abrupt rupture of the thin water meniscus due to the thermodynamic instability of the liquid-vapor interface, and (iii) mechanical manipulation of the thin aqueous column by repeated stretch-relaxation cycles, revealing the atomic-scale contact angle hysteresis.

Water molecules in ambient conditions produce a nanoscale water meniscus between a hydrophilic Si tip and a hydrophilic mica substrate, when capillary condensation occurs as the stiff AFM tip approaches the substrate within a nanometric distance (Fig. 1). Once the thin aqueous column is formed, it is stretched vertically upward by subsequent retraction of the tip. As the molecular water bridge of subzeptoliter (zepto $= 10^{-21}$) volume is elongated, the force gradient associated with the elasticity of the system is thereby measured by an extremely small amplitude-modulation operation of AFM [7,8].

Figure 1 presents the schematics of a home-built AFM setup used for formation of a nanometric water column by capillary condensation as well as for simultaneous measurement of the force gradient of the elongated water meniscus, obtained at a given relative humidity (RH) and at room temperature (21 °C). A small-radius Si tip [NSG series by NT-MDT, (100) oriented with a typical radius of 10 nm], presumably having a nanometric discrete structure of atomic layers [9,10] in the ambient condition, is glued on a high-frequency $f_0 (= 1\,002\,198$ Hz) quartz crystal oscillator that has a very high stiffness $k_0 (\approx 5.4 \times 10^5$ N/m) and quality factor $Q (\approx 10^4)$. These parameters, under ambient conditions, allow the tip to be operated in extremely small amplitude-modulation (≈ 0.01 nm), noncon-

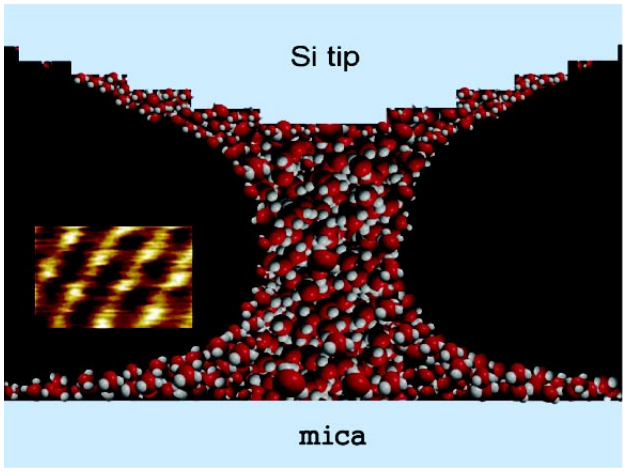

FIG. 1 (color online). Experimental schematics of a high sensitivity AFM setup operating in ambient conditions. The inset shows an atomic-resolution AFM image of a dry and clean mica substrate, obtained at a modulation-amplitude change of 5% (scan area: 1.5 nm × 1 nm) [6].

tact, scanning mode suitable for high-resolution force-gradient measurement.

In contrast to a conventional micro-fabricated cantilever-based AFM used either in contact or noncontact mode, our AFM tip is stiff enough to pull the condensed water molecules without colliding with the substrate, as well as sensitive enough to measure the small changes of the force gradient (≈ 0.1 N/m). The minimum detectable force gradient of our detection scheme is estimated to be about 0.05 N/m. For control of RH, some desiccant material was placed inside a metallic enclosure containing the AFM. Measurements were made only when the RH, accurately monitored within 2% error by a digital hygrometer, was slowly decreased down to a desired value after several hours. Moreover, since our AFM did not employ a laser for the force-gradient measurement, there was very low electric power dissipation (<1 nW) so that the local temperature variations near the tip were almost negligible.

In dynamic force microscopy, an oscillating probe detects the force gradient between the tip and sample along its oscillation direction. Such force gradient detected by the probe, $k_{ts} = -\partial F_{ts}/\partial z$, is related to the resonance frequency shift (Δf) by [8]

$$k_{\mathrm{ts}} = -\frac{\partial F_{\mathrm{ts}}}{\partial z} = 2k_0 \frac{\Delta f}{f_0}. \tag{1}$$

In our small-amplitude-modulation operation of AFM, however, one has to convert the measured amplitude change to the frequency change in order to obtain the force gradient. We have measured such a response curve, which shows that the resonance frequency of the tuning fork decreases by 10 Hz as the amplitude decreases by 5%. Thus, Δf is related to $\Delta A (\equiv A - A_0)$ by

$$\Delta f \approx \frac{10}{0.05}\left(\frac{\Delta A}{A_0}\right), \tag{2}$$

where A is the oscillation amplitude during approach or retraction, and A_0 is the free oscillation amplitude of the tuning fork. Here the measured frequency shift is negative, indicating that the force gradient is also negative or the interaction force is attractive [11].

Figure 2 presents experimental results of the force-gradient measurement: magnitude of the force gradient versus elongation of the water column, obtained at a given RH of [Fig. 2(a)] 2%, [Fig. 2(b)] 15%, [Fig. 2(c)] 31%, and [Fig. 2(d)] 45%. Each set of data represents one single approach (blue empty triangles) and retraction (red filled circles) process obtained at a given RH. The origin in Fig. 2(a) represents the tip-substrate contact point, whereas it denotes the position of tip retraction in Fig. 2(b) to Fig. 2(d). The approaching tip is computer-controlled to retract immediately after its modulation amplitude is decreased by $\approx 1\%$ due to the effects of capillary-induced damping, which keeps the water meniscus as thin as possible. This was important because the initial width and volume of the meniscus depended much upon the rapidity

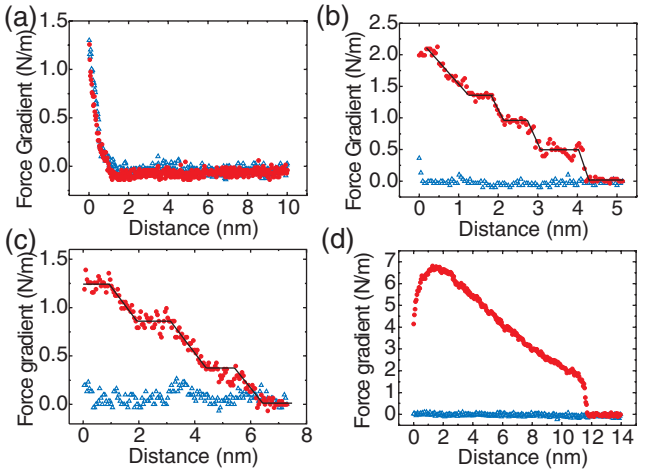

FIG. 2 (color). Measured values of the force gradient of the water meniscus as a function of its elongation at a given RH of (a) 2%, (b) 15%, (c) 31%, and (d) 45%. The approach and retraction speed is 0.15 nm/s. The black solid line in (b) and (c) is a guide to the eye.

of the tip retraction after the abrupt development of capillary condensation.

In a very dry condition of Fig. 2(a), the measured elastic force gradient showed no noticeable hysteresis behaviors during the tip approach and retraction. The force gradient of ≈ 1 N/m near the tip-substrate contact was due to the typical short-range (<1 nm) adhesive forces and the van der Waals forces between the tip and the substrate. Therefore, the absence of hysteresis as well as the atomic-resolution noncontact AFM image of the mica substrate (inset of Fig. 1) indicated that there was neither capillary condensation of water nor any binding materials in between the tip-substrate gap. This was expected because the mica sample was placed, after *in situ* cleavage and subsequent chemical cleansing with dilute acid [12,13], inside an airtight enclosure. In particular, the experimental results of the force-gradient measurements did not show any noticeable dependence on whether the substrate was chemically treated or not, indicating the insensitivity to any possible surface contaminants or impurities. Note that the Si tip, attached to the crystal resonator, was treated by ultrasound cleansing in ethyl alcohol anhydrous before use in the experiment.

At 15% RH, on the other hand, similar measurements showed quite different results [Fig. 2(b)]. As the tip approached the substrate, the force gradient increased abruptly as a result of the strongly attractive capillary forces arising from the Laplace pressure as well as the surface tension of condensed water [14]. Such capillary condensation occurred at less than ≈ 1 nm tip-substrate distance [2,15], at which there was negligible tip-surface interaction in dry conditions [see Fig. 2(a)]. Moreover, as can be observed in Fig. 2(b), the elastic force gradient decreased stepwise as the tip retracted. There appeared three distinct steps (although the initial retraction region

of 1.2 nm may as well be regarded as two additional steps) before the force gradient vanished (i.e., the water column was ruptured) at the distance of 4.2 nm from the retraction position. In particular, there was obvious regularity in the step heights (0.45 ± 0.03 N/m) as well as in the step-plateau lengths (0.6 or 1.2 nm). Moreover, the rupture was found to occur abruptly within a distance of 0.1 nm, as manifested by the steep step edge. Similar values of the plateau lengths as well as the step heights were also obtained at different approach or retraction speeds of the tip: for example, at an approach speed of 0.01 nm/s and retraction speed of 1.23 nm/s, we have observed the plateau lengths of 0.6 to 1 nm and the step heights of 0.5 to 0.6 N/m.

The discreteness of the force gradient may be associated with the atomic-scale stick slip behavior [16] of the three-phase (i.e., tip-vapor-liquid) circular contact line developed on the tip surface. The contact line is pinned at the atomic step position of the discretely layered structures of the curved Si tip surface (Fig. 1) [9,10], because Si atoms at the step edge with low bond-coordinate number exert extra attractive pinning forces on the water molecules. Once such a pinning process occurs, the magnitude of the force gradient in the vertical direction remains constant during subsequent stretch of the water column, like an elastic linear spring, as manifested by the plateau in Figs. 2(b) and 2(c).

While the surface area of the constant-volume water column increases as the tip retracts, the contact angles with respect to the tip surface as well as the Laplace pressure are decreased steadily [14]. Then a slip of the contact line occurs when the water column is stretched enough so that the contact angle becomes equal to a critical value, beyond which the pinning energy can no longer compensate for the extra surface energy needed in maintaining the same contact position. The force gradient decreases rather abruptly during the slip process and the slip stops when the contact angle restores its equilibrium value at the next atomic step position of the tip where the free energy is minimized. It is interesting that similar stepwise decrease with respect to elongation was observed in the measurement of the quantized conductance of a nanometric gold junction formed between two gold surfaces [17], which was shown to be highly correlated with the stiffness change of the metallic nanocontact [18].

The area under the last plateau before the rupture (≈ 600 pN) represents the capillary force at the last stick position of ≈ 3.1 nm. The corresponding work done until the rupture occurs (≈ 2.3 eV) is approximately equivalent to the overall loss of tens of hydrogen bonds during the last 1 nm elongation. A simple estimate of the meniscus-neck diameter, given the vertical force of 600 pN, presents a value of ≈ 2.6 nm, assuming the bulk value for the surface tension of the water-air interface (72.8 mN/m at 20 °C). The additional contribution of the Laplace pressure to the force, on the other hand, was negligible before the rupture, which resulted in only a slight reduction of the estimated neck diameter. Such an ultrathin water meniscus with ≈ 5 nm in length [Fig. 2(b)] corresponds to a cylindrical liquid volume of $\approx 10^{-20}$ cm^3 (or 10 yoctoliter), consisting of only $\sim 10^3$ water molecules. As the meniscus thins even more, the relative fluctuation of the liquid-vapor interface increases so that the meniscus becomes thermodynamically unstable [19]. The observed rupture of the meniscus occurs when the neck has a width of ≤ 2.6 nm and this critical value is in agreement with the simulation results [20]. Such interfacial instability also manifests itself as an increased level of fluctuations of the measured force gradient in the last plateau before the rupture [Fig. 2(b)].

The results at 31% RH [Fig. 2(c)], which were independently obtained with the same tip on a different day, showed overall steplike discrete characteristics similar to those in Fig. 2(b), except that the step edges following the plateaus were broader (0.9 ± 0.1 nm). At a higher RH of 45% [Fig. 2(d)], however, the elasticity-distance curves exhibited smooth variations except for the final rupture process, as similarly observed in Ref. [21]. The continuous and monotonic decrease of the elastic-force gradient as well as the much larger initial values of the force gradient indicated that the water meniscus was already of bulklike nature before the tip retraction, smearing out the stepwise discrete changes [22]. In other words, as the initial amount of capillary-condensed water increased due to the uniform water layer formed on the mica substrate at an RH higher than 40% [2], the contact circle became larger in diameter and the effective pinning strength was diminished, resulting in the usual steady sliding of bulk water. The broadened step edges shown in Fig. 2(c) may be caused by mixed effects of the stick slip and the steady sliding behaviors.

Note that the elasticity measurements in Fig. 2 were performed during a single approach-retraction process after the RH reached a desired value, in order to avoid any unwanted ''memory'' effects of the water meniscus as well as to form the thinnest possible meniscus width. On the other hand, similar force-gradient measurements, performed after more rapid (at 1 nm/s) and repeated (30 times) cycles were executed, showed very different behaviors: a longer plateau (~ 10 nm) appeared both in the approach and retraction curves, before the rupture at a much larger force gradient (~ 10 N/m) occurred. This observation may be associated with the fact that a bulklike meniscus with a submicrometer-scale thickness [23] was produced due to the tip being dipped repeatedly in a microscopic water droplet formed on the mica substrate [24].

To confirm that the measured force gradient during approach and retraction of the tip truly represented the mechanical elasticity of the system, and to explore the potential of the present technique for manipulation of the nanometric aqueous column, we repeatedly stretched and relaxed the water column by a slow (0.15 nm/s speed) cyclic motion of the tip. Figure 3(a) shows an approach-retraction curve, which was obtained when the approach-

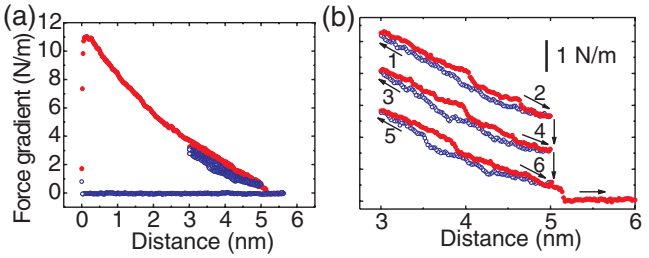

FIG. 3 (color). Reproducibility of the repeated short-ranged approach-retraction cycles of the force-gradient measurement, obtained at 13% RH. (a) The tip makes a deeper initial approach followed by repetitive cycles of retraction and approach until the water bridge is intentionally ruptured. (b) Close-up plot of the repeated cycles, with an arbitrary vertical offset for an eye guide. The approach and retraction speed of the tip is 0.15 nm/s.

ing tip retracts as soon as its initial modulation amplitude is now decreased by ≈10%, resulting in a ''closer'' approach with respect to that in Fig. 2(b) obtained at a similar RH. The repeated cycles then start when the tip retracts from the origin up to ≈5 nm distance just before the rupture, and continue within the subsequent 2 nm range.

Figure 3(b) presents a close-up plot of the repeated cycles shown in Fig. 3(a), with an arbitrary vertical offset given between each cycle just for a clear eye guide. The vertical scale bar represents the force gradient of 1 N/m. The tip movement is in the order of the increasing arrow number. The retraction curve of the last cycle (arrow #6) is followed by an intentional rupture of the thin water column. The evident reproducibility of the repeated cycles in Fig. 3(b) indicates that the force-gradient measurements indeed reveal the elastic properties of the ultrathin water column. In particular, the repeated hysteresis behaviors within each cycle are indicative of the atomic-scale contact angle hysteresis of the nanometric water column on the tip surface [16], which is closely related to the atomic-scale friction.

The present work may provide a novel experimental tool for studying the kinematics of the condensed or adsorbed liquids on the surfaces, which is of fundamental and technological interest in surface science and engineering [25]. One can also study water molecules in nanoconfinement [26] that may behave unexpectedly by forming nanoclusters or by rearranging themselves to seek the energetically most favorable configurations by bending, but not breaking, the finite hydrogen-bonded network [27]. Furthermore, the current technique to form and manipulate a nanometric water column between two surfaces may provide a means to extend our understanding of the transport processes of ions through a nanometric water channel in biological cells.

We are grateful to H. E. Stanley, S. Buldyrev, J. Yu, Y.-W. Son, K. Kim, M. H. Lee, and J. Jang for helpful discussions. This work was supported by the Korean Ministry of Science and Technology through Creative Research Initiatives Program.

*Corresponding author.
Email address: whjhe@snu.ac.kr

[1] U. Raviv, P. Laurat, and J. Klein, Nature (London) **413**, 51 (2001).
[2] J. Hu, X.-D. Xiao, D. F. Ogletree, and M. Salmeron, Science **268**, 267 (1995).
[3] J. N. Israelachvili, P. M. McGuiggan, and A. M. Homola, Science **240**, 189 (1988).
[4] G. Hummer, J. C. Rasaiah, and J. P. Noworyta, Nature (London) **414**, 188 (2001).
[5] P. G. Kusalik and I. M. Svishchev, Science **265**, 1219 (1994).
[6] Y. Seo, H. Choe, and W. Jhe, Appl. Phys. Lett. **83**, 1860 (2003).
[7] R. Garcia and R. Perez, Surf. Sci. Rep. **47**, 197 (2002).
[8] F. J. Giessibl, Rev. Mod. Phys. **75**, 949 (2003).
[9] T. Arai and M. Tomitori, J. Vac. Sci. Technol. B **18**, 648 (2000).
[10] T. Arai and M. Tomitori, Appl. Phys. Lett. **86**, 073110 (2005).
[11] D. Sarid, *Scanning Force Microscopy with Applications to Electric, Magnetic and Atomic Forces* (Oxford University Press, New York, 1994), 2nd ed., p. 22.
[12] M. M. Kohonen and H. K. Christenson, Langmuir **16**, 7285 (2000).
[13] U. Raviv and J. Klein, Science **297**, 1540 (2002).
[14] J. N. Israelachvili, *Intermolecula and Surface Forces* (Academic, New York, 1994).
[15] L. Sirghi, Appl. Phys. Lett. **82**, 3755 (2003).
[16] P. G. de Gennes, Rev. Mod. Phys. **57**, 827 (1985).
[17] A. I. Yanson, G. R. Bollinger, H. E. van den Brom, N. Agrait, and J. M. van Ruitenbeek, Nature (London) **395**, 783 (1998).
[18] R. Budakina and S. J. Putterman, Appl. Phys. Lett. **81**, 2100 (2002).
[19] J.-G. Weng, S. Park, J. R. Lukes, and C.-L. Tien, J. Chem. Phys. **113**, 5917 (2000).
[20] J. Jang, G. C. Schatz, and M. A. Ratner, Phys. Rev. Lett. **90**, 156104 (2003).
[21] L. Zitzler, S. Herminghaus, and F. Mugele, Phys. Rev. B **66**, 155436 (2002).
[22] O. M. Braun and J. Röder, Phys. Rev. Lett. **88**, 096102 (2002).
[23] M. Schenk, M. Futing, and R. Reichelt, J. Appl. Phys. **84**, 4880 (1998).
[24] L. Xu, A. Lio, J. Hu, D. F. Ogletree, and M. Salmeron, J. Phys. Chem. B **102**, 540 (1998).
[25] R. D. Piner, J. Zhu, F. Xu, S. Hong, and C. A. Mirkin, Science **283**, 661 (1999).
[26] S.-H. Park and G. Sposito, Phys. Rev. Lett. **89**, 085501 (2002).
[27] M.-C. Bellissent and J. C. Dore, *Hydrogen Bond Networks*, NATO ASI, Ser. C, Vol. 435 (Kluwer Academic Publishers, Dordrecht, 1994).